Journal of Food and Nutrition Research, 2024, Vol. 12, No. 11, 471-481
Available online at http://pubs.sciepub.com/jfnr/12/11/1
Published by Science and Education Publishing
DOI:10.12691/jfnr-12-11-1

Cissus Qadrangularis (L.) Stem Loaded Solid Lipid Nanoparticles Stimulate Osteogenic Differentiation Via Bone Morphogenic Protein-6 and Runt-related Transcription Factor 2 (RUNX2) in Human Mesenchymal Stem Cells

P. Subash-Babu[*], Nada Al Saran, Ali A Alshatwi[*]

Department of Food Science and Nutrition, College of Food and Agricultural Sciences,
King Saud University, P. O. Box 2460, Riyadh-11451, Saudi Arabia
*Corresponding author: alshatwi@ksu.edu.sa, subash@ksu.edu.sa

Received September 28, 2024; Revised October 30, 2024; Accepted November 06, 2024
[*]*These authors contributed equally to this work*

Abstract The current study aimed to explore the role of *Cissus quadrangularis* (L.) stem on osteogenic differentiation of human mesenchymal stem cells (hMSCs) and their application in bone regeneration. Orally administered natural products and its bioactive compounds often results in poor absorption, low solubility, and restricted bioavailability due to their vulnerability to intestinal hydrolytic and enzymatic degradation. To overcome these challenges, bioactive compounds extracted from C. *quadrangularis* were fabricated into solid lipid nanoparticles (CQ-SLNp) to enhance bioavailability. MTT assay confirmed that the CQ-SLNp found with safe and significantly increased hMSCs proliferation and IC_{25} was identified. The impact of CQ-SLNp on stimulation of osteogenic differentiation in hMSCs at the lowest concentration was evaluated and compared to osteogenic standard medium alone after 4, 10 and 14 days, according to alkaline phosphatase (ALP) activity and alizarin red staining (ALZ) analysis. Bone morphogenic protein-receptor (BMPr) and Runt-related transcription factor 2 (RUNX2) associated mRNA levels has been analyzed. CQ-SLNp increased ALZ intensity and ALP activity. BMPr, RUNX2 and Wnt/β-catenin expressions found to be increased in osteogenesis induced hMSCs after 10 days compared to negative control. Although, the osteogenic differentiation was more effective in CQ-SLNp treatment when compared to CQ alone treated cells. We observed enhanced osteogenesis in CQ-SLNp alone treated hMSCs than standard differentiation medium. Taken together, the observed finding suggests that CQ-SLNp exhibited bioavailability and induced osteogenic differentiation of hMSCs, indicative of their potential applications for bone remodeling applications.

Keywords: *Osteoarthritis, C. quadrangularis, solid lipid nanoparticles, bone morphogenic factors, osteogenesis*

Cite This Article: P. Subash-Babu, Nada Al Saran, and Ali A Alshatwi, "*Cissus Qadrangularis* (L.) Stem Loaded Solid Lipid Nanoparticles Stimulate Osteogenic Differentiation Via Bone Morphogenic Protein-6 and Runt-related Transcription Factor 2 (RUNX2) in Human Mesenchymal Stem Cells." *Journal of Food and Nutrition Research*, vol. 12, no. 11 (2024): 471-481. doi: 10.12691/jfnr-12-11-1.

1. Introduction

Osteoarthritis (OA) is a common bone and joint disease, characterized by progressive loss of articular cartilage, osteophyte dysfunction, abnormal osteocyte differentiation and loss of joint function [1]. Osteocytes make up 95% of bone cells and play roles in responding to mechanical forces developing cracks due to mechanical stress and osteonecrosis. The death of osteocytes triggers bone restructuring by promoting the formation of bone tissue through the activation of cells that break down bone (osteoclasts) and cells that build bone tissue (osteoblasts) which release a protein called sclerostin that leads to bone resorption [2]. In addition, osteoarthritis (OA) recognized with the physiological conditions such as osteophyte formation, features of bone sclerosis, cyst in subchondral bone, articular cartilage, and synovium tissues [3]. A formation of organic matric or cysts surrounded by less bone density bone uncoupled with calcification may suggest spatially differential regulation of osteoblasts and osteoclasts by Wnt/β-catenin signaling and the RUNX2 pathway [4]. Sclerostin inhibited Wnt signaling, inhibit osteoblastic activity and terminate bone remodeling cycle [5].

Bone remodeling modulation might suppress osteophyte formation, improve progressive loss in cartilage and decreased bone marrow lesions (BMLs) in

human OA [6]. Osteogenic differentiation ability has been achieved successfully in human mesenchymal stem cells (hMSCs) isolated from several tissue sources, especially from bone marrow [7]. MSCs differentiation into osteoblasts, osteoprogenitor cells which develop into osteo-precursors upon upregulation of Runx2 (Runt related transcription factor 2), bone marphogenic proteins (BMPs) and Wnt signaling. Proliferation and maturation of osteocytes begin with early-osteoblasts lineages and osteogenic precursors form osteoblasts [8].

Phytochemicals from plant owing their health benefits, such as carnosine, berberine, catechin increased the osteogenic differentiation *in vitro* and *in vivo* [9]. Wu et al. [10] have identified the natural compounds such as ginsenoside, icartin and hydroxycholesterol have identified with osteogenic potentials with low toxicity and high utility. In addition, zingerone [from ginger] stimulate the bone transcription factor, Runx2 in hMSCs [11] and naringin [active component of Rhizoma drynariae] stimulate osteogenic differentiation and anti-osteoporotic properties in the osteoblast cell line [12]. Most of the secondary metabolites from plants have been failed in further drug development, due to challenges such as poor absorption, low solubility, and limited bioavailability particularly when administered orally. These difficulties arise from susceptibility of natural products and their bioactive compounds to intestinal hydrolytic and enzymatic degradation. Currently the applications of solid lipid nanoparticles (SLNp) as carriers, enabling the bioavailability through effective absorption of active metabolites such as triptolide, metformin, silymarin, berberine, and pomegranate extract with pharmacological potential are most successful [13,14,15,16]. In this context, Icariin loaded nanoplatform effectively enhance osteogenesis and bone regeneration when compared to free icariin [17,18]. Khezri et al. [19] confirmed that the curcumin-containing nanoscaffolds enhancing the cellular and molecular mechanisms behind the osteogenic differentiation from mesenchymal stem cells (MSCs).

Cissus quadrangularis L. belongs to the grape family which is also known as veldt grape, adamant creeper, or devil's backbone. It has been used to relieve pain and mend bone fractures from the ancient time [20]. *C. quadrangularis* has been demonstrated to help decrease joint pain and arthritis symptoms. It improved exercise-induced joint discomfort with chronic joint pain in humans [21]. Furthermore, *C. quadrangularis* was more successful in reducing swelling and decreasing inflammation than typical pharmaceuticals used to treat rheumatoid arthritis [22]. Potu et al. [23] confirmed that the *C. quadrangularis* exhibited higher proliferation, differentiation and calcification rates which confirms the osteoblasts (osteoblastogenesis) and extracellular matrix calcification in bone marrow mesenchymal stem cells undergo osteogenic stimulation. In the present study, based on the above literature we aimed to identify and entrap the phytochemicals of *C. quadrangularis* L. with phosphatidylcholine and hyaluronic acid to improve the intracellular uptake, bioavailability and approached as efficient drug deliver to stimulate osteocyte differentiation and maturation signaling pathway to prevent osteoarthritis.

2. Materials and Method

Chemicals

Hyaluronic acid, dimethyl sulfoxide (DMSO), phosphatidylcholine, MTT [3-(4,5-dimethyl-2-thiazolyl)-2,5-diphenyl-2h-tetrazolium bromide], hydrogen peroxide (H_2O_2) were purchased from Sigma chemical company (St. Louis, MO, USA). Cell staining agents such as ethidium bromide, propidium iodide, acridine orange and mitochondrial stain, jc-1 (MMP assay) were also purchased from Sigma-Aldrich (St. Louis, MO, USA). Cell growth media, phosphate buffered saline (PBS), fetal bovine serum (FBS) and molecular biology-related chemicals were obtained from Gibco chemicals (Grand Island, NY), USA.

Plant material

C. quadrangularis L. (veldt grape) and *Salvia hispanica* L. (chia seed) were procured from iHerbs and Spices in Riyadh, Saudi Arabia. The identification and authentication of the plant names and species were carried out by Taxonomist (Dr. V. Duraipandiyan, Professor, Department of Botany, College of Science, King Saud University, Riyadh). The plant specimen for *C. quadrangularis* L. (CQ) and KSU-SH-07 for *Salvia hispanica* L., (SH) were deposited and displayed in public herbarium, King Saud University, Riyadh-11451.

Extraction

C. quadrangularis L. and *Salvia hispanica* L. underwent shade drying, and grinding using a commercial blender, respectively. A quantity of 400 gm of CQ powder was immersed in 1200 ml of laboratory grade methanol for 72 hr, the content was kept in a mechanical shaker. Following the 72 hr period, the phytoconstituents bound with methanol were collected by filtration and reconstituted using a rotary evaporator. The concentrated CQ extract (CQE) underwent filtration, then subsequently stored at -20ºC until needed for further use. Following this, 200 gm of *Salvia hispanica* L. seed powder were extracted with ethyl acetate to extract phospholipids. The extraction progress of *Salvia hispanica* L. seeds have been carried out as same as the CQ seed progress.

Chemical analysis using GC-MS

CQ and SH extracts were assessed using gas chromatography (GC) coupled with a 5975 inert mass-spectrometer (MSD) [Agilent 7890A, Agilent Technologies, USA]. GC-MS column featured with 30m length, 0.25mm inner diameter, and 0.25µm film thickness, a Triple-Axis detector (MSD) and a liquid sampler. Pure LS or SH extracts (1 ml) subsequently injected, employing a split ratio of 30:1, respectively. The initial temperature was fixed at 280°C and the column temperature was maintained at 300°C throughout the analysis. Helium, operating at a flow rate of 1mL/min, served as the carrier gas. The electron ionization energy was set as 70 eV. Data collection occurred post full-scan mass spectra within the 40-550 AMU scan range. The LS or SH constituents were then quantified based on peak area percentage.

Formulation solid lipid nanoparticle containing C. quadrangularis L. seed

Chia seed phospholipids were employed as the lipid phase during the formulation of solid lipid nanoparticles

(SLNp) according to solvent emulsification evaporation method. In brief, a lipid phase mixture comprising chia seed phospholipids (15 µL), phosphatidylethanolamine (10 µL), hyaluronic acid and 25mg of CQ extract (CQE) were dissolved in 20 ml acetone and melted on a hot plate equipped with a water bath, surpassing its melting point. Simultaneously, a surfactant solution, containing stabilizing agents like Tween 20 and lecithin, was prepared in an aqueous phase (30 ml). The molten chia seed phospholipid was emulsified with the surfactant solution to form a pre-emulsion. High-pressure ultrasonication was then applied to reduce particle size, resulting in the creation of solid lipid nanoparticles. The nanoemulsion was allowed to cool, leading to the solidification of lipid nanoparticles. The final SLNp formulation underwent characterization for crucial parameters, including particle size and polydispersity index, to ensure optimal performance and stability.

Characterization of prepared CQ-SLNp

Total drug content in CQ phytocomponents loaded CQ-SLNp was quantified from 1 mL of freshly prepared CQ-SLNp using a spectrophotometer at 420 nm. Presence of functional chemical interaction were analyzed using FT-IR (Agilent, USA). Using Zetasizer (NANO-Zs90) the particle size was determined and dynamic light scattering (DLS) technique used to calculate the z-average diameter. The morphology, shape, size, and morphology of CQ-SLNp were analyzed using high-resolution scanning electron microscopy (SEM, JEOL, Japan). Negative staining with 2% uranyl acetate (w/v) was employed against sample.

Cell lines and cell culture

Present study, the hMSCs cells were purchased from ATCC (American type culture collections, USA). Cells were cultured in a humidified atmosphere with 5% CO_2 at 37°C using DMEM (Dulbecco's Modified Eagle's medium) enriched with 10% FBS (fetal bovine serum), 2 mM $_L$-glutamate and 1% penicillin/ streptomycin (antibiotics) as growth medium. Upon reaching 80% confluence, growth media was removed and trypsinized using 0.25% trypsin/EDTA solution. Further, the cell pellets were collected following centrifugation at 3500 rpm for 5 min at room temperature. The corresponding cell numbers were seeded onto 96, 24, or 6 wells plate for MTT assay, staining and gene expression analysis.

MTT assay

Following appropriate culture conditions with the confirmation of 80% confluence, the cells were subjected to MTT assay. The MTT (3-(4,5-dimethylthiazol-2-yl)-2,5-diphenyltetrazolium bromide) assay was carried out in hMSCs (growing in osteogenic differentiation medium) to assess the effect of CQE (0, 5, 10, 20, 40, 80, 160 µg/mL) and CQ-SLNp (0, 2, 4, 8, 16, 32, and 64 µg/mL) on neither inhibition nor enhance the cell viability after day-1, day-5 and day 10. Viable cells tend to convert the soluble dye (yellow) into insoluble formazan crystals (purple), which were subsequently solubilized using DMSO. The absorbance was measured spectrophotometrically at 570 nm, providing a quantitative representation of cell viability. The number of viable cells has been calculated in percentage according to the mean value of the sample/control absorbance × 100.

Alkaline phosphatase Assay

In a 96-well plate, CQE (20 and 40 µg/mL) and CQ-SLNp (4 and 8 µg/mL) were treated to osteogenic differentiation induced hMSCs, respectively. 80 µL of condition medium (on 4^{th} and10^{th} days) was mixed with 20 µL of 0.75 M 2-amino-2-methyl-1-propanol buffer and 100 µL of 10 mM *p*-nitrophenylphosphate solution and incubated for until color development. Earlier, 0.2 M NaOH was added to arrest the conversion of *p*-nitrophenylphosphate to *p*-nitrophenol. Absorbance was measured in a spectrophotometer at 450 nm.

Mineralization

After the cytotoxicity assay, 20 and 40 µg/mL dose of CQE and 4 and 8 µg/mL dose of CQ-SLNp were selected as effective and safe dose to study the mineralization during osteogenic differentiation. The cells were then analyzed for calcium production at 10 and 14 days by staining with 10% Alizarin red solution (the dye specifically binds to calcium). Followed by fixation, the staining cells were washed three times with PBS and the fixed stains were eluted using 1mL of 10% cetylpyridium chloride (Sigma) were added to each well and incubated for 20 min. To quantify the stain accumulation, 100µL of this eluted stain was utilized to read at 550nm using a microplate reader [24]. A standard curve has been prepared using Alizarin Red stain and cetylpyridium chloride. The calcium deposition was expressed as molar equivalent of calcium. One mole of Alizarin Red binds to two moles of calcium in an Alizarin Red S-calcium complex.

JC-1 Staining assay

Mitochondrial membrane potential was measured in bone cell stem cells that were undergoing differentiation on the 4th and 10th days of the process. The cells exposed to CQE and CQ SLNp were treated with JC 1 dye for 20 minutes at 37°C, in an environment. After staining the cells were rinsed to get rid of dye. Examined under a fluorescence microscope. Changes in color, from green (indicating membrane potential) to red (indicating high mitochondrial membrane potential) showed the status of mitochondria and images were taken for record keeping purposes. 500 stained cells were randomly selected for analysis and the mitochondrial membrane potential was manually calculated with images captured during the process.

Gene expression analysis

Total RNA and cDNA were synthesized using Fastlane® cell cDNA kit from control, CQE (20 and 40 µg/mL) and CQ-SLNp (4 and 8 µg/mL) treated cells (7500 Fast Real-Time PCR System, Applied Biosystems, USA). The genes corresponding to the osteogenic differentiation, such as RUNX2 (Runt-related transcription factor 2), BMP-2 (bone morphogenetic protein-2), BMP-4, COL1A1 (collagen 1A1), VDR-1 (vitamin D receptor), ALPL (alkaline phosphatase) were quantified on 4^{th} day. In addition, the gene associated with osteoblast signaling and maturation, such as FRZ-2 (Frizzled protein 2), Wnt 5a, β-catenin related mRNA were quantified on 14^{th} day against the reference gene, β-actin by the method of Yuan et al [25]. All the primers were purchased from Qiagen, and sequence were verified in primer-BLAST, National Library of Medicine, online software and OriGene Global, Rockville, MD 20850, USA. The qPCR was performed using 25µL reaction volume and 40 cycles were allowed for amplification

using Applied Biosystems 7500 Fast Real-Time PCR System (USA). Two negative controls were included for each gene by removing template cDNA. The relative expression levels were calculated by the formula: ΔΔCt (comparative threshold) = amplification values of CQE or CQ-SLNp treated (ΔCt) - ΔCt (positive control). The amplification of each target was normalized to its corresponding mRNA levels of β-actin using the $2^{\Delta\Delta Ct}$ method using Applied Biosystems software.

Quantification of protein using ELISA

On 10th day, the amount of osteocyte differentiation and maturation related proteins such as, SPARC (osteonectin), SPP1 osteopontin (OPN or bone /sialoprotein I (BSP-1 or BNSP), *SPP1* (secreted phosphoprotein 1), BGLAP (osteocalcin or bone gamma-carboxyglutamic acid-containing protein in control, CQE (µg/mL) and CQ-SLNp (8 µg/mL) treated cells using high-sensitivity ELISA-kits (Quantikine, R&D Systems, Minneapolis, MN, USA). The assay kits detect both soluble and receptor-bound proteins and thus measures the total concentration of proteins. The values were expressed as pg/mg protein for all the analyzed proteins.

Statistical analysis

The experimental data was analyzed by one-way analysis of variance (ANOVA). Then post-hoc analysis with Tukey's range test was carried out to compare and analyze the data within and between the groups using SPSS/28.5 software package (IBM, New York, USA). For all the comparisons, differences were considered statistically significant at $p \leq 0.05$ and $p \leq 0.001$ [26].

C. quadrangularis L. extract phytochemical profiling

The methanol extract of *C. quadrangularis* L. has been extensively analyzed using Gas Chromatography Mass Spectrometry (GC-MS) have been presented in Figure 1. The analysis revealed a range of compounds with biological activities, including antimicrobial, antioxidant, anticancer and anti-inflammatory effects. Some notable compounds identified in the analysis include acid methyl ester, benzyl nitrile, 2,3,5,6-tetrafluoroanisole and 3 isoquinolinamine. The presence of these compounds may contribute to the extract's biological potential. The presence of phytochemicals in *C. quadrangularis* L. highlights its value and supports its traditional use in different therapeutic applications. Detailed information about the constituents of this plant has been presented in Table 2.

Characterization of prepared CQ-SLNp

Physiochemical characterization of the solid lipid nanoparticles (SLNp) loaded with *C. quadrangularis* L. (CQ) extract using various analytical techniques. In SEM, we carefully examined the CQ SLNp and observed particle size between 76 to 125 nm (Figures 2A and 2B). These images provided insights into the surface structure and morphology of the nanoparticles allowing us to better understand their properties. Particle size analysis revealed that the nanoparticles exhibited a distribution with a size of 65nm (Figures 2C and 2D). This uniformity in size distribution is crucial for ensuring their effectiveness and suitability, for applications indicating a well-controlled synthesis process.

3. Results

Table 1. Primer sequences used in quantitative real-time polymerase chain reaction (RT-PCR)

Gene	Forward Primer (5' to 3')	Reverse Primer (5' to 3')
RUNX-1	CGGTTACCTTACACCCGCA	TGGTCTGGTGGTGGTGAAG
BMP-2	GCTGCTAACTTTCGCTGTCG	GAACTTCTCGGCAGCCAGTA
BMP-4	AGCGGACTGAGAAAAGGAGTTC	TGAAGCGCCGTTCTTCTTCT
COL1A1	GAGGGCCAAGACGAAGACATC	CAGATCACGTCATCGCACAAC
ALPL	ACCATTCCCACGTCTTCACATTTG	AGACTGCGCCTGGTAGTTGTTGT
VDR	AGCTGGCCCTGGCATTGTA	ATGGCAGCAGGGGAAGAAAG
FRZ-2	TCCAGGAAAGACAACCCTGA	GGTCTCCACAGTGCTGTTGT
Wnt 5a	GAGTGGAGCGTGGTATGGT	CGGTTGTTGCTGATGCTGTC
β-catenin	TCAGGCTTATGCTGGACCA	GACTTGAGCTTGCCACTCAG

Table 2. GC-MS phytochemical profiling of *C. quadrangularis* L. methanol extract (CQME) showing the similarity in the database

Peak number	List of compounds	Molecular formula	Molecular weight	Reported biological activity
1	Benzoic acid (methyl ester)	$C_8H_8O_2$	136.052	Antimicrobial [27]
2	Benzyl nitrile	C_8H_7N	117.058	Stimulants [28]
3	3-Isoquinolinamine	$C_9H_8N_2$	144.069	Antimicrobial [29]
4	5-(hydroxymethyl)-2-Furancarboxaldehyde	$C_6H_6O_3$	126.032	Anti-inflammatory and anticancer [30]
5	6-Aminotetrazolo(b) pyrid azine	$C_4H_4N_6$	136.05	Not found
6	Isothiocyanatomethyl benzene	C_8H_7NS	149.03	Antimicrobial [31]
7	Benzene acetamide	C_8H_9NO	135.068	Antimicrobial [32]
8	Anhydro-1,6- β-D-Glucopyranose	$C_6H_{10}O_5$	162.053	Antioxidant [33]
9	2,3,5,6-Tetrafluoroanisole	$C_7H_4F_4O$	180.02	Anticancer [34]
10	3-(3,4,5-trimethoxyphenyl)- 2-Propenoic acid	$C_{13}H_{15}N_3O_5$	238.084	Antileishmanial [35]
11	9,12,15-Octadecatrien-1-ol	$C_{18}H_{32}O$	264.245	Antioxidant [36]
12	2-dimethylaminoethyl ester- 4-Butylbenzoic acid	$C_{19}H_{30}O_2$	249.173	Antifungal [37]
13	9-Octadecenamide	$C_{18}H_{35}NO$	281.272	antioxidative and hypolipidemic [38]

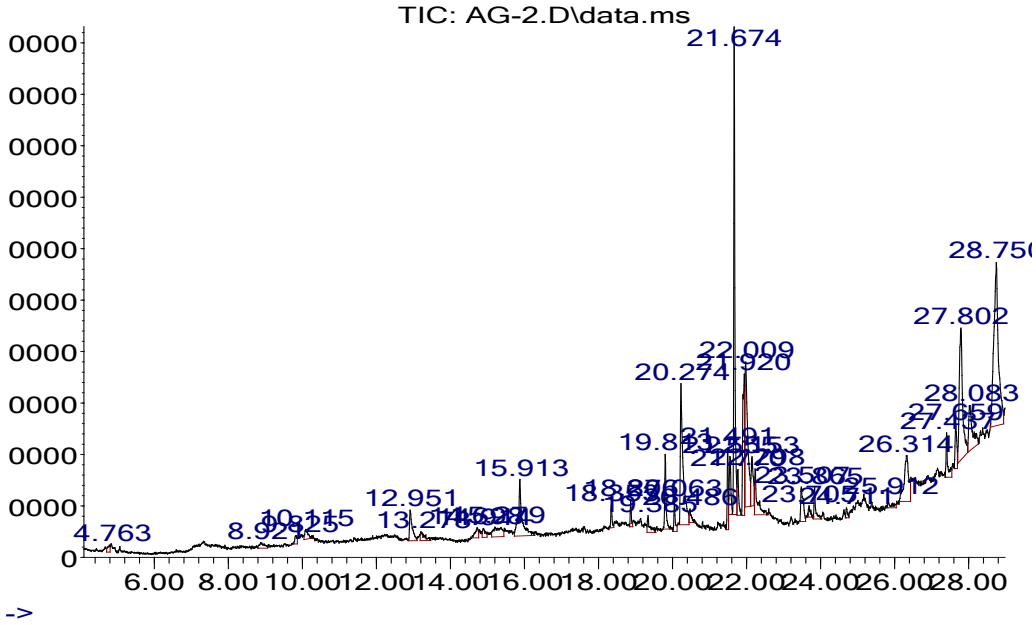

Figure 1. Gas chromatography- mass spectrum (GC-MS) chromatogram for *C. qadrangularis*. L. methanol extract

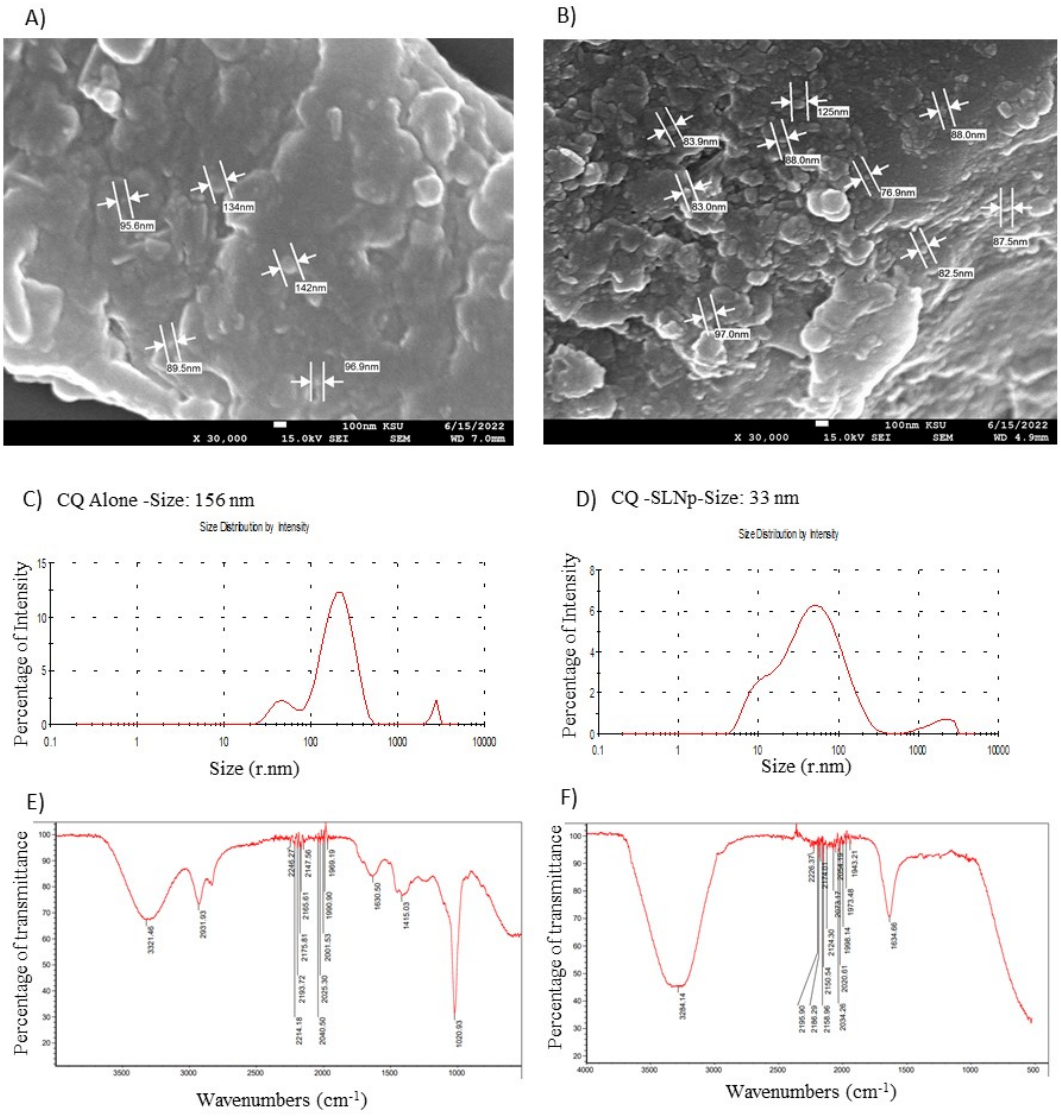

Figure 2. Characterization of *C. quadrangularis* L. alone (lA, 1C, 1E) and *C. quadrangularis* L. loaded solid lipid nanoparticle (CQ-SLNp) (1B, 1D, 1F) using scanning electron microscopy (SEM) (1A, 1B), particle size (1C, 1D) and FT-IR (1E, 1F) analysis

Fourier Transform Infrared Spectroscopy (FT-IR) analysis played a role in distinguishing the characteristics of the CQ extract and the CQ loaded SLNp (as shown in Figures 2E and 2F) revealing significant differences in their spectra. CQ Extract: The spectrum displayed peaks at 3321.46, 2931.93 and 2246.27cm^{-1} along with a wide absorption band ranging from 3500 to 2000cm^{-1}. The peaks such as 1630.50, 1020.93 and 1415.03 cm^{-1} were observed only in CQE. CQ loaded SLNp; This was characterized by peaks at 3284.14 cm^{-1} featuring a pattern beyond 3500 cm^{-1} and specific peaks at 2195.90, 2186.29, 2158.96 and 2226.37cm^{-1}. Furthermore, new peaks were detected at wavelengths as; 2124.30, 2073.17, 2054.19, 2034.26, 2020.61cm^{-1} and 1998.14, 1973.48 and 1943.21cm^{-1}. The comparative analysis emphasized variations in % transmittance between the spectra of the CQ extract and the CQ loaded SLNp indicating changes in composition after encapsulation process took place. The presence of peaks in the CQ loaded SLNp spectrum implies modifications or interactions during the solid lipid phase encapsulation process that might influence the effectiveness and functionality of these nanoparticles. The FT IR analysis has provided evidence that the encapsulation process was successful. This is evident, from the chemical profiles and the presence of peaks in the spectrum of CQ-SLNp compared to the CQ extract. These differences highlight the changes in groups and potential modifications in chemical composition that occur during encapsulation.

Cell Viability Assessment

The undifferentiated hMSCs were cultured in 10% FBS containing growth medium for 48 hr, after confluence the characterization osteogenic differentiation was carried out. The undifferentiated hMSCs were cultured in basic growth medium showed negative to ALP activity and Ca^{2+} deposition negative in Alizarin red staining. While the hMSCs cultured in osteogenic differentiation media, the Alizarin red staining found with high red accumulation confirmed the Ca^{2+} accumulation and osteogenic differentiation. In addition, we found increased ALP activity after day 10.

To ensure that either CQE or CQ-SLNp did not compromise cell health cell viability was assessed. The hMSCs cultured in osteogenic differentiation medium were treated with increasing concentration of CQE (0, 5, 10, 20, 40, 80, 160 µg/mL) and CQ-SLNp (0, 2, 4, 8, 16, 32, and 64 µg/mL). The cell growth stimulation was extensive between day 1 to day 10 when compared to the untreated hMSCs on day 1 (Figure 3-i) or day 10 (Figure 3-ii). The cell proliferation was increased on day 5, after day 5 no further increase of the cell number was identified.

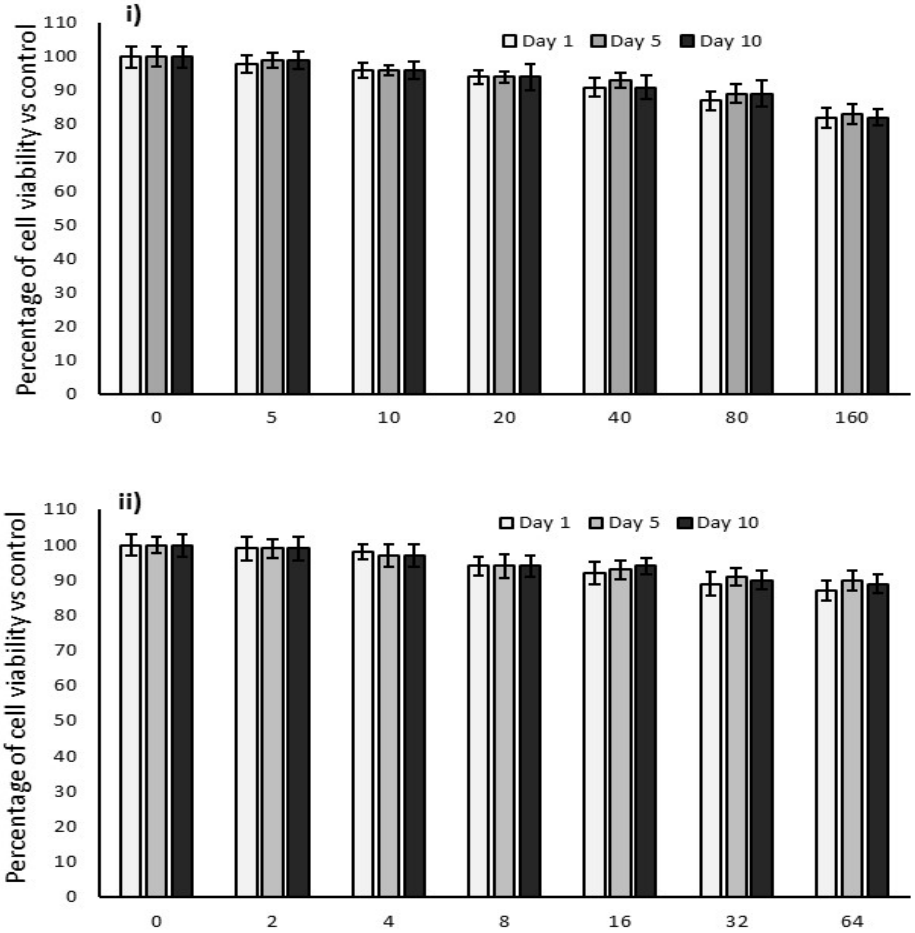

Figure 3. Effect of increasing concentration of *C. quadrangularis* L. extract (0, 5, 10, 20, 40, 80 and 160 µg/mL) [3-i] and *C. quadrangularis* L. loaded solid lipid nanoparticle (CQ-SLNp) (0, 2, 4, 8, 16, 32, and 64 µg/mL) [3-ii] on cell viability across a Span of day-1, day 5 and day-10. Data are displayed as the SD ± deviation (n = 6). No significance

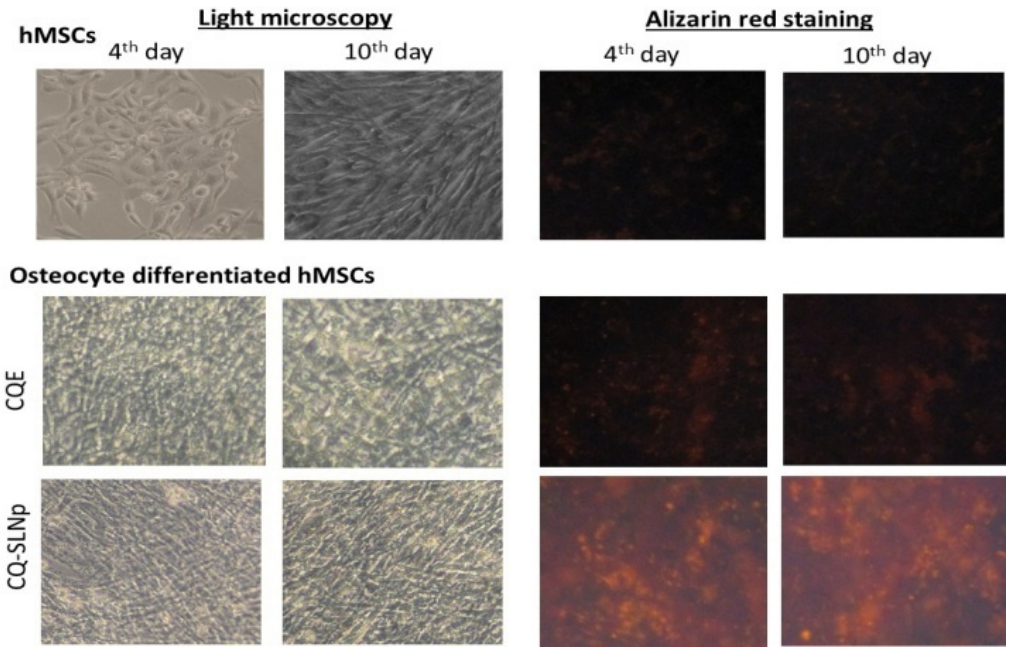

Figure 4. Comparative Analysis of Osteocyte Differentiation and Mineralization in hMSCs by light Microscopy and Alizarin Red Staining after 10 Days

Alizarin Red Staining Test and Alkaline Phosphatase

Analysis using Alizarin Red staining revealed that both the CQ and CQ-SLNp treatments effectively promoted calcium deposition in the matrix indicating maturation. The CQ treatment resulted in an increase in mineralization at 40 µg/mL when compared to 20 µg/mL or the control group. However, the CQ-SLNp group exhibited mineral deposition with staining intensity three times greater than that of the control group. The lower dose (4/ml) of CQ-SLNp was found with 2 times greater mineral deposition, it was significantly ($p \leq 0.001$) higher than the higher dose of CQE (Figure 4).

The ALP test showed that both the CQ and CQ-SLNp treatments significantly increased ALP activity both in 4th and 10th day when compared to the control group. However, the CQ-SLNp group exhibited the increase in ALP activity indicating an effect on osteogenic differentiation. Specifically, cells treated with 40 µg/mL of CQ showed significantly higher level of ALP activity in 10th day when compared to 4th day (Figure 5-i). CQ-SLNp at 8 µg/mL treatment showed significantly increased level of ALP even at 4th day; further on 10th day 2-fold increase was observed when compared to the untreated control (Figure 5-ii).

Mitochondrial Potential Assay

JC-1 staining was done to check the health of the mitochondria. Cells treated with CQ-SLNp showed JC-1 formation indicating that the mitochondrial membrane potential was maintained, a sign of healthy and metabolically active cells. Additionally, the DAPI nuclear staining confirmed the cell viability showing that treatment, with CQ-SLNp led to an improvement, in integrity and density (Figure 6).

Quantitative polymerase chain reaction (qPCR) analysis

The analysis using polymerase chain reaction (qPCR) aimed to understand the gene expression profiles associated with stress, inflammation, nerve cell proliferation and osteogenic differentiation. The experimental results were compared the control group, with groups treated with CQ and CQ-SLNp. Osteogenesis and osteocyte maturation related genes expressions levels were compared between CQE (40 µg/mL) and CQ-SLNp (8 µg/mL) treated cells on 4th day (osteogenic inducer) and 10th day (maturation).

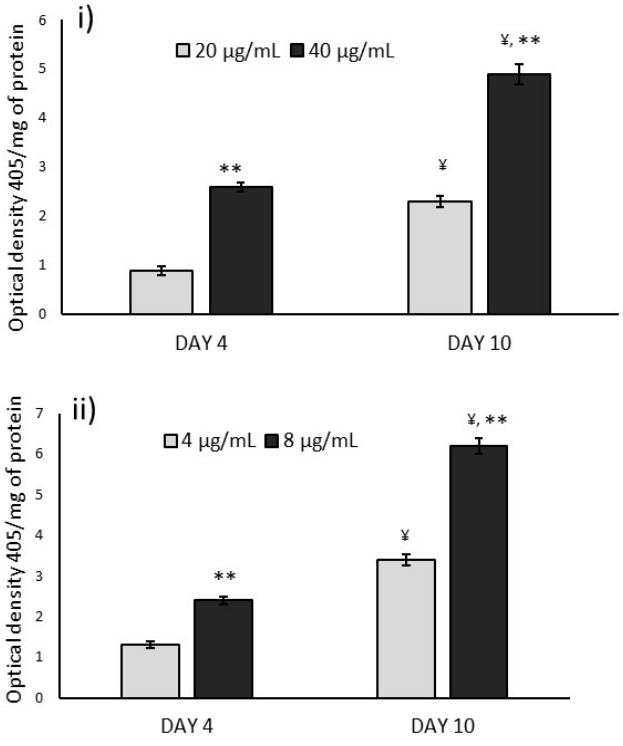

Data is shown as a change ALP levels compared between to the CQ and CQ-SLNp. The results are displayed as the SD ± deviation (n = 6). * Indicates significance at $p \leq 0.05$ while ** denotes significance at $p \leq 0.001$ compared to the CQ.

Figure 5. Assessing osteocyte development through ALP activity levels with CQ (i) [20, 40 µg/mL) and CQ-SLNp (ii) [4, 8 µg/mL] on Days 4 and 10

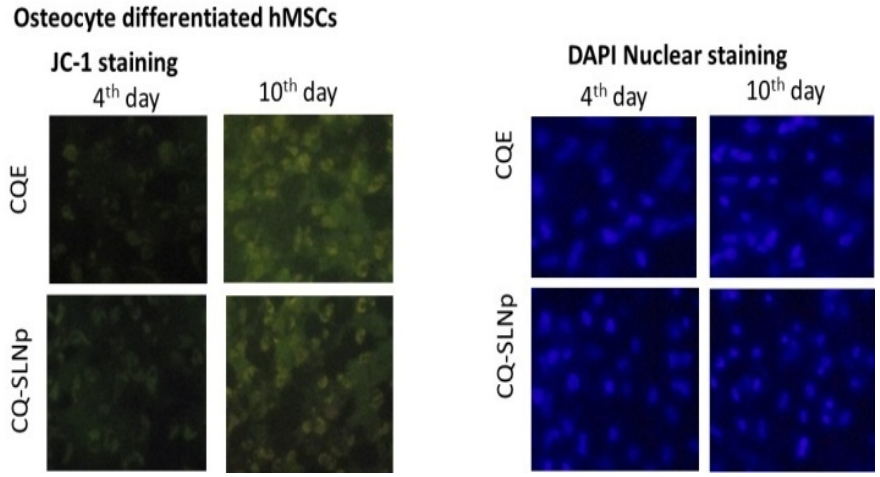

Figure 6. Mitochondrial membrane potential (JC-1) and Nuclear Integrity (DAPI Staining) in differentiated osteocyte after 10 Days

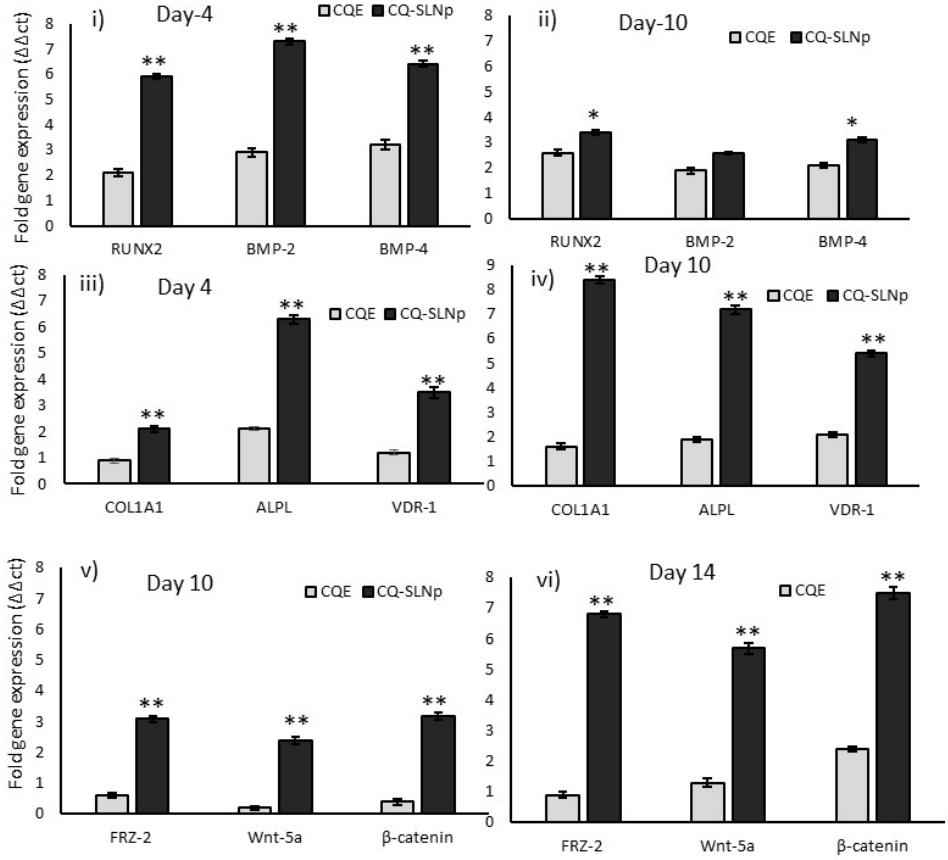

Figure 7. Changes in the gene expression of osteogenic differentiation markers osteogenic inducer (i, ii) on day-4, osteogenesis stimulator (iii,iv) on day-10 and Osteogenesis maturation (day-10 and 14) linked signaling pathway associated traits (v, vi) components in CQ and CQ-SLNp treated cells

In the early 4th day, most of the hMSCs were differentiated into osteocyte have been confirmed by the increased osteogenic inducer mRNA expression such as in the Figure 7 (i, ii) as, RUNX-1, BMP-2, BMP-4 up-to 3-fold when compared to CQE alone treated differentiation induced hMSCs. Meanwhile on the 10th day, the up-regulated expression of osteogenic inducer genes was inclining to normal level in both CQE or CQ-SLNp treated cells.

The expression levels of osteogenesis stimulator markers, such as in the Figure 7 (iii, iv) as COLA1, ALPL and VDR-1 expression have been significantly ($p \leq 0.05$) increased on 4th day, but during 10th day the expression levels were increased upto 3-fold when compared to CQE treated cells.

Osteogenesis maturation linked signaling pathway associated traits such in the Figure 7 (v, vi) as, FRZ-2, Wnt-5a and β catenin were significantly ($p \leq 0.001$) increased to 3-fold in the CQ-SLNp group after 10 days when compared to early 4th day expression. In CQE treated cells, the expressions of FRZ-2, Wnt-5a and β catenin were found to be non-significant in 4th day; but on 10th day the expression level found to be significant ($p \leq 0.01$).

Protein expression

The results for osteocyte differentiation signaling and

maturation associated protein levels showed that both CQE (40 µg/mL) and CQ-SLNp (8 µg/mL) treated cells effectively increased SPARC (osteonectin), SPP1 osteopontin (OPN or bone /sialoprotein I (BSP-1 or BNSP), Wnt-5a, BGLAP (osteocalcin or bone gamma-carboxyglutamic acid-containing protein on 10th day when compared to 4th day (Figure 8-i). In addition, we observed a significantly ($p \leq 0.001$) decreased levels of oxidative stress (such as LPO, NOX-2) and pro inflammatory genes (such as IL1β, TNF-α) during the 10th day. Overall, the cells treated with CQ-SLNp exhibited a significantly higher reduction in this stress and inflammatory markers. This suggests that the nanoparticle formulation has osteogenesis, anti-inflammatory and anti-oxidative effects (Figure 8-ii).

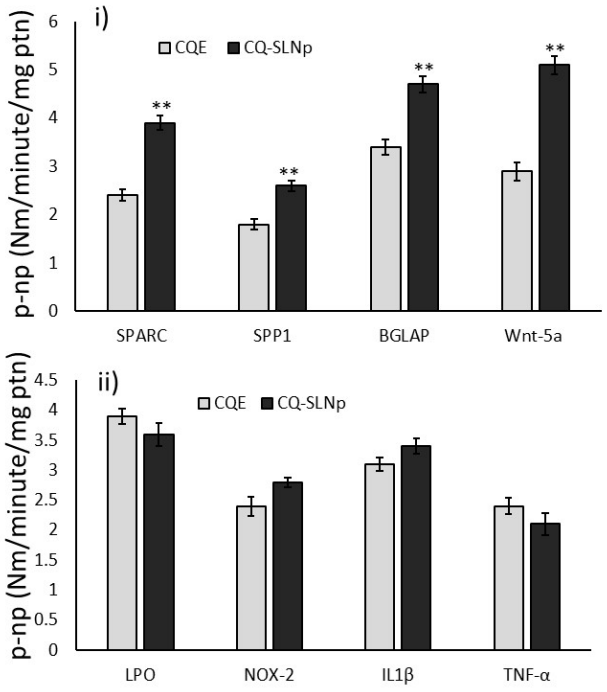

The activity is measured as the rate of p nitrophenol (p np) production per minute per milligram of protein (Nm/min/mg protein). Results are shown as mean ± deviation. ** $p \leq 0.001$ compared to CQ treatment

Figure 8. Assessment of protein levels associated with inflammatory markers in cells treated with CQ and CQ-SLNp; (i) Demonstrates enzyme activity levels for SPARC, SPP1, BGLAP and Wnt 5a markers. (ii) Illustrates enzyme activity levels for LPO, NOX-2, IL1β and TNF-α markers

4. Discussion

Our investigation findings indicate that the use of *C. quadrangularis* stem loaded lipid nanoparticles (CQ-SLNp) can potentially enhance the process of osteocyte differentiation from human mesenchymal stem cells (hMSCs). This enhancement is evident through an increase in alkaline phosphatase activity and mineral accumulation confirmed by Alizarin Red S staining, well as the heightened expression of key markers associated with osteogenesis, such as bone morphogenic protein receptor (BMPr) and Runt related transcription factor 2 (RUNX2). These results suggest that CQS SLNs possess a capacity to induce bone formation potentially by activating signaling pathways related to osteogenesis.

The role of *C. quadrangularis* promoting the regeneration of bone has been well documented despite the bioavailability and solubility challenges it presents. In this context, Zahan et al [39] who demonstrated that *C. quadrangularis* has the potential to accelerate the healing of bone in rat models. This study has enabled us to progress to deliver compounds from *C. quadrangularis* with lipid nanoparticles (SLNs). In addition, nanoencapsulated drug delivery for improved drug availability and osteocyte formation [40, 41].

Our research extensively explores the mechanisms for osteogenic differentiation. We specifically focus on the enhancement of BMPr and RUNX-2 gene expression. In this context Chen et al [42] and Lee et al [43] have confirmed the importance of RUNX2, which is considerd as a major differentiation regulator for osteogenesis. RUNX2 emphasize its role in promoting differentiation and facilitating the bone formation process [42,43]. Additionally, the function of RUNX2 including its involvement in various signaling pathways and regulation of gene transcription, during osteoblast development have been confirmed [44,45]. By integrating these perspectives our findings provide an understanding of the processes involved in bone formation highlighting the significant contributions made by BMPr and RUNX2 within this field. We provide insights by employing SLN technology to address the bioavailability challenges of *C. quadrangularis* thereby enhancing its capabilities for applications in bone tissue engineering [46]. In addition, studies conducted by Parvathi [47] and Tamburaci [48] has explored the phytochemicals of CQ and their role in promoting differentiation and bone regeneration with a focus, on the advantages it offers for the functions of mesenchymal stem cells.

Our study aligns, with research that emphasizes the role of the Wnt/β catenin signaling pathway in osteogenesis bone remodeling and osteoblast differentiation [49]. We also delve into the use of lipid nanoparticles loaded with *C. quadrangularis* stem extracts (CQ-SLNp) for promoting bone growth when compared to free CQ extract. This exploration provides insights into harnessing nanoparticle modified extracts to facilitate bone regeneration. The Wnt/β catenin pathway is vital for bone development and it plays a role in maintaining bone balance. Impaired Wnt/β catenin pathways are associated with conditions like osteoporosis and osteogenesis imperfecta (OI) [50] and the maintenance of bone mass [51]. Activation of this pathway promotes bone formation while its inhibition can lead to a reduction in bone density [52]. However, it's worth noting that targeting this pathway for purposes needs consideration due to potential risks such as tumorigenesis [53]. Furthermore, Stohs and Ray [54] validate the efficacy of *C. quadrangularis* in promoting bone formation and facilitating the healing of fractures. Many studies emphasize the plants potential to enhance bone growth especially when utilized alongside SLN technology to enhance bioavailability [55,56]. Our findings highlight the benefits of utilizing nanoparticle technology to enhance the effectiveness of herbal extracts in promoting optimal bone health. This represents an advancement in integrating medicine with contemporary therapeutic strategies.

The osteogenic differentiation observed significantly

higher in CQ-SLNp treatment is likely mediated through the synergistic actions of BMP-6 and RUNX2 upregulation and Wnt/β-catenin pathway activation [6,57,58]. These pathways are known to be pivotal for the initiation and progression of osteoblast differentiation, as well as for the maturation of osteocytes, providing a mechanistic basis for the observed enhancement in osteogenesis [59]. The utilization of nanoparticles in therapies focused on regenerating bone has the potential to address limitations in treatments for bone related disorder [60]. Nanotechnology offers applications in engineering bone tissue, including targeted delivery of molecules and growth factors scaffold construction and cell labeling when compared to free supplementation of drug [61]. These applications can augment the differentiation process of bone cells and support tissue regeneration [62]. In relation to osteoporosis combining nanomaterials within a scaffold holds promise for localized and long-term treatment options [63]. Overall incorporating nanoparticles into bone regeneration therapies presents an approach with potential, for improving treatment outcomes.

5. Conclusion

This research emphasizes the potential of using lipid nanoparticles made from *C. quadrangularis* (CQ SLNp) to enhance the process of bone formation in human mesenchymal stem cells (hMSCs) through increased bioavailability and bio efficacy. By improving differentiation of osteocyte and increasing the expression of markers for bone formation CQ-SLNp proves to be more effective compared to traditional methods used for bone development, such as *C. quadrangularis* extracts alone. These findings highlight the novel and efficient approach that CQ-SLNp offers for regenerating bones, which was considered as a step ahead towards addressing conditions like failure in targeted drug delivery or loss of bioavailability. Further studies are necessary to optimize the formulation of CQ-SLNp, for its application thus advancing medicine and the field of bone tissue engineering.

Conflict of Interest Statement: The authors declare that there is no conflict of interest.

Author Contribution: NA conducted the analysis and drafted the original manuscript. P.S-B developed the methodology. AA re-vised the manuscript. P.S-B and AA reviewed, edited, and approved the final manuscript.

Data Availability: The data presented in this study are available on request from the corresponding author.

Acknowledgement: This research was funded by the Researchers Supporting Project number (RSP2024R178), King Saud University, Riyadh, Saudi Arabia.

References

[1] Hemmatian H, Bakker AD, Klein-Nulend J, van Lenthe GH. Aging, Osteocytes, and Mechanotransduction. In Current Osteoporosis Reports 2017; 15(5).

[2] Henriksen K, Neutzsky-Wulff AV, Bonewald LF, Karsdal MA. Local communication on and within bone controls bone remodeling. In Bone 2009; 44(6).

[3] Chiba K, Nango N, Kubota S, Okazaki N, Taguchi K, et al. Relationship between microstructure and degree of mineralization in subchondral bone of osteoarthritis: A synchrotron radiation μCT study. Journal of Bone and Mineral Research 2012; 27(7).

[4] Palumbo C, Ferretti M. The osteocyte: From “prisoner” to “orchestrator.” In journal of functional morphology and kinesiology 2021; 6(1).

[5] Ten Dijke P, Krause C, De Gorter DJJ, Löwik CWGM, Van Bezooijen R L. Osteocyte-derived sclerostin inhibits bone formation: Its role in bone morphogenetic protein and Wnt signaling. Journal of bone and joint surgery 2008; 90(1).

[6] Ling L, Dombrowski C, Foong KM, Haupt LM, Stein GS, et al. Synergism between Wnt3a and heparin enhances osteogenesis via a phosphoinositide 3-kinase/Akt/RUNX2 pathway. Journal of biological chemistry, 2010; 285(34).

[7] Matta C, Szűcs-Somogyi C, Kon E, Robinson D, Neufeld T, et al. Osteogenic differentiation of human bone marrow-derived mesenchymal stem cells is enhanced by an aragonite scaffold. Differentiation 2019; 107.

[8] Maes C, Kobayashi T, Selig MK, Torrekens S, Roth SI, et al. Osteoblast precursors, but not mature osteoblasts, move into developing and fractured bones along with invading blood vessels. Developmental cell 2010; 19(2).

[9] Sharifi S, Moghaddam FA, Abedi A, Maleki Dizaj S, Ahmadian S, et al. Phytochemicals impact on osteogenic differentiation of mesenchymal stem cells. In BioFactors 2020; 46(6).

[10] Wu Y, Liu Y, Xu Y, Zheng A, Du J, Cao L, Shi J, Jiang X. Bioactive natural compounds as potential medications for osteogenic effects in a molecular docking approach. Frontiers in pharmacology 2022; 13, 955983.

[11] Srinaath N, Balagangadharan K, Pooja V, Paarkavi U, Trishla A, Selvamurugan, N. Osteogenic potential of zingerone, a phenolic compound in mouse mesenchymal stem cells. BioFactors (Oxford, England) 2019; 45(4), 575–582.

[12] Zhang P, Dai KR, Yan SG, Yan WQ, Zhang C, Chen DQ, Xu B, Xu ZW. Effects of naringin on the proliferation and osteogenic differentiation of human bone mesenchymal stem cell. European journal of pharmacology 2009; 607(1-3), 1–5.

[13] Badawi N, El-Say K, Attia D, El-Nabarawi M, Elmazar M, Teaima M. Development of pomegranate extract-loaded solid lipid nanoparticles: quality by design approach to screen the variables affecting the quality attributes and characterization. ACS Omega 2020; 5(34), 21712–21721.

[14] Bharali DJ, Siddiqui IA, Adhami VM, Chamcheu JC, Aldahmash AM, Mukhtar H, Mousa SA. Nanoparticle delivery of natural products in the prevention and treatment of cancers: Current status and future prospects. In cancers 2011; 3(4).

[15] Mohseni R, Arabsadeghabadi Z, Ziamajidi N, Abbasalipourkabir R, Rezaeifarimani A. Oral administration of resveratrol-loaded solid lipid nanoparticle improves insulin resistance through targeting expression of snare proteins in adipose and muscle tissue in rats with type 2 diabetes. Nanoscale research letters 2019; 14: 227.

[16] Xue M, Zhang L, Yang MX, Zhang W, Li XM, et al. Berberine-loaded solid lipid nanoparticles are concentrated in the liver and ameliorate hepatosteatosis in db/db mice. International journal of nanomedicine 2015; 10.

[17] Bose S, Sarkar N. Natural Medicinal Compounds in Bone Tissue Engineering. Trends in biotechnology 2020; 38(4): 404–417.

[18] Mohammadzadeh M, Zarei M, Abbasi H, Webster TJ, Beheshtizadeh N. Promoting osteogenesis and bone regeneration employing icariin-loaded nanoplatforms. Journal of biological engineering 2024; 18(1): 29.

[19] Khezri K, Maleki DS, Rahbar Saadat Y, Sharifi S, Shahi S, Ahmadian E, Eftekhari A, Dalir Abdolahinia E, Lotfipour F. Osteogenic Differentiation of Mesenchymal Stem Cells via Curcumin-Containing Nanoscaffolds. Stem cells international 2021; 1520052.

[20] Brahmkshatriya H, Shah K, Ananthkumar G, Brahmkshatriya M. Clinical evaluation of *Cissus quadrangularis* as osteogenic agent in maxillofacial fracture: A pilot study. AYU (An International Quarterly Journal of Research in Ayurveda) 2015; 36(2).

[21] Bloomer RJ, Farney TM, McCarthy CG, Lee SR. *Cissus quadrangularis* reduces joint pain in exercise-trained men: a pilot study. The physician and sports medicine 2013; 41(3).

[22] Bhujade A, Talmale S. In vivo studies on antiarthritic activity of *Cissus quadrangularis* against adjuvant induced arthritis. Journal of Clinical & Cellular Immunology 2015; 6(03).

[23] Potu BK, Bhat KM, Rao MS, Nampurath GK, Chamallamudi MR, Nayak SR, Muttigi MS. Petroleum ether extract of *Cissus*

quadrangularis (Linn.) enhances bone marrow mesenchymal stem cell proliferation and facilitates osteoblastogenesis. Clinics (Sao Paulo, Brazil) 2009; 64(10): 993–998.

[24] Nørgaard R, Kassem M, Rattan SIS. Heat shock-induced enhancement of osteoblastic differentiation of hTERT-immortalized mesenchymal stem cells. Annals of the new york academy of sciences 2006; 1067 (1).

[25] Yuan JS, Reed A, Chen F, Stewart CN. Statistical analysis of real-time PCR data. BMC Bioinformatics 2006; 7.

[26] Kim H.-Y. Analysis of variance (ANOVA) comparing means of more than two groups. Restorative dentistry & endodontics 2014; 39(1).

[27] Charnock C, Finsrud T. Combining esters of para-hydroxy benzoic acid (parabens) to achieve increased antimicrobial activity. Journal of clinical pharmacy and therapeutics 2007; 32(6).

[28] Mishra DK, Dhote V, Bhatnagar P, Mishra PK. Engineering solid lipid nanoparticles for improved drug delivery: Promises and challenges of translational research. In drug delivery and translational research 2012; 2(4).

[29] Galán A, Moreno L, Párraga J, Serrano Á, Sanz MJ, et al. Novel isoquinoline derivatives as antimicrobial agents. Bioorganic and medicinal chemistry, 2013; 21(11).

[30] Xia M, Liu L, Qiu R, Li M, Huang W, et al. Anti-inflammatory and anxiolytic activities of *Euphorbia hirta* extract in neonatal asthmatic rats. AMB Express 2018; 8(1).

[31] Rathish IG, Javed K, Ahmad S, Bano S, Alam MS, et al. Synthesis and antiinflammatory activity of some new 1,3,5-trisubstituted pyrazolines bearing benzene sulfonamide. Bioorganic and medicinal chemistry letters 2009; 19(1).

[32] Ju L, Bode JW. Amide Formation by decarboxylative condensation of hydroxylamines and α-Ketoacids: N -[(1 S)-1 Phenylethyl]-Benzeneacetamide . In organic syntheses. 2010; 87: 218–225.

[33] Zhang DQ, Tan XF, Tian H, Liu QM, Peng WX. Pyrolysis-GC/MS determination of biomedical components of the pyrolyzate from fruit hull and kernel hull of *Camellia oleifera* fruit. 2nd International Conference on Bioinformatics and Biomedical Engineering (ICBBE) 2008.

[34] Wu YQ, Peng WX, Song Y, Qing Y, Li S, He W. Determination of biomedicine components of *Dinochloa puberula* McClure by Py-GC/MS. 2nd International Conference on Bioinformatics and Biomedical Engineering (ICBBE) 2008.

[35] Mondal S, Rahaman CH. Studies in pharmacognostic characters of the climber *Erycibe paniculata* Roxb. of Convolvulaceae. Journal of medicinal plants studies 2020;8(2).

[36] Hossain MA, Al-Toubi WAS, Weli AM, Al-Riyami QA, Al-Sabahi JN. Identification and characterization of chemical compounds in different crude extracts from leaves of Omani neem. Journal of taibah university for science 2013; 7(4).

[37] Adebiyi JA, Njobeh PB, Adebo OA, Kayitesi E. Metabolite profile of Bambara groundnut (*Vigna subterranea*) and dawadawa (an African fermented condiment) investigation using gas chromatography high resolution time-of-flight mass spectrometry (GC-HRTOF-MS). Heliyon 2021; 7(4).

[38] Cheng MC, Ker YB, Yu TH, Lin L, Peng RY, Peng CH. Chemical synthesis of 9(Z)-octadecenamide and its hypolipidemic effect: A bioactive agent found in the essential oil of mountain celery seeds. Journal of agricultural and food chemistry 2010; 58(3).

[39] Zahan MN, Hasan M, Mallik S, Hashim MA, Juyena NS. Effect of *Cissus quadrangularis* on fracture healing in laboratory animal. Journal of health & biological sciences 2022; 10(1).

[40] Hajiali H, Ouyang L, Llopis-Hernandez V, Dobre O, Rose FRAJ. Review of emerging nanotechnology in bone regeneration: Progress, challenges, and perspectives. In Nanoscale 2021; 13(23).

[41] Cheng H, Chawla A, Yang Y, Li Y, Zhang J, Jang HL, Khademhosseini A. Development of nanomaterials for bone-targeted drug delivery. In Drug Discovery Today 2017; 22(9).

[42] Chen G, Deng C, Li YP. TGF-β and BMP signaling in osteoblast differentiation and bone formation. In international journal of biological sciences 2012; 8(2).

[43] Lee K-S, Kim H-J, Li Q-L, Chi X-Z, Ueta C, et al. Runx2 is a common target of transforming growth factor β1 and bone morphogenetic protein 2, and cooperation between Runx2 and Smad5 induces osteoblast-specific gene expression in the pluripotent mesenchymal precursor cell line C2C12. Molecular and Cellular Biology 2000; 20(23).

[44] Lian JB, Javed A, Zaidi SK, Lengner C, Montecino M, et al. Regulatory controls for osteoblast growth and differentiation: Role of Runx/Cbfa/AML Factors. In critical reviews in eukaryotic gene expression 2004; 14(1–2).

[45] Schroeder TM, Jensen ED, Westendorf JJ. Runx2: A master organizer of gene transcription in developing and maturing osteoblasts. In Birth Defects Research Part C - Embryo Today: Reviews 2005; 75(3).

[46] Mohseni R, Arabsadeghabadi Z, Ziamajidi N, Abbasalipourkabir R, Rezaeifarimani A. Oral administration of resveratrol-loaded solid lipid nanoparticle improves insulin resistance through targeting expression of snare proteins in adipose and muscle tissue in rats with Type 2 Diabetes. Nanoscale research letters 2019; 14: 227.

[47] Parvathi K, Krishnan AG, Anitha A, Jayakumar R, Nair MB. Poly(L-lactic acid) nanofibers containing *Cissus quadrangularis* induced osteogenic differentiation in vitro. International journal of biological macromolecules 2018; 110.

[48] Tamburaci S, Kimna C, Tihminlioglu F. Novel phytochemical *Cissus quadrangularis* extract–loaded chitosan/Na-carboxymethyl cellulose–based scaffolds for bone regeneration. Journal of bioactive and compatible polymers 2018; 33(6).

[49] Hong G, He X, Shen Y, Chen X, Yang F, et al. Chrysosplenetin promotes osteoblastogenesis of bone marrow stromal cells via Wnt/β-catenin pathway and enhances osteogenesis in estrogen deficiency-induced bone loss. Stem cell research and therapy 2019; 10(1).

[50] Baron R, Kneissel M. WNT signaling in bone homeostasis and disease: from human mutations to treatments. In nature medicine 2013; 19(2).

[51] Monroe DG, McGee-Lawrence ME, Oursler MJ, Westendorf JJ. Update on Wnt signaling in bone cell biology and bone disease. In Gene 2012; 492(1).

[52] Liu X, Kim JH, Wang J, Chen X, Zhang H, et al. Wnt signaling in bone formation and its therapeutic potential for bone diseases. In therapeutic advances in musculoskeletal disease 2013; 5(1).

[53] Hoeppner LH, Secreto FJ, Westendorf JJ. Wnt signaling as a therapeutic target for bone diseases. In expert opinion on therapeutic targets 2009; 13(4).

[54] Stohs SJ, Ray SD. A review and evaluation of the efficacy and safety of *Cissus quadrangularis* extracts. Phytother research 2013; 27(8): 1107-14.

[55] Rao MS, Bhagath KP, Narayana SVB, Gopalan KN. *Cissus quadrangularis* plant extract enhances the development of cortical bone and trabeculae in the fetal femur. Pharmacologyonline 2007; 3.

[56] Gaur T, Lengner CJ, Hovhannisyan H, Bhat RA, Bodine PVN, et al. Canonical WNT signaling promotes osteogenesis by directly stimulating Runx2 gene expression. Journal of biological chemistry 2005; 280(39).

[57] Brahmkshatriya HR, Shah KA, Ananthkumar GB, Brahmkshatriya MH. Clinical evaluation of *Cissus quadrangularis* as osteogenic agent in maxillofacial fracture: A pilot study. Ayuurvedic 2015; 36(2): 169-73.

[58] Mbalaviele G, Sheikh S, Stains JP, Salazar VS, Cheng SL, et al. β-catenin and BMP-2 synergize to promote osteoblast differentiation and new bone formation. Journal of cellular biochemistry 2005; 94(2).

[59] Hess K, Ushmorov A, Fiedler J, Brenner RE, Wirth T. TNFα promotes osteogenic differentiation of human mesenchymal stem cells by triggering the NF-κB signaling pathway. Bone 2009; 45(2).

[60] Filippi M, Born G, Felder-Flesch D, Scherberich A. Use of nanoparticles in skeletal tissue regeneration and engineering. Histology and histopathology 2020; 35(4).

[61] Walmsley GG, McArdle A, Tevlin R, Momeni A, Atashroo D, et al. Nanotechnology in bone tissue engineering. In Nanomedicine: Nanotechnology, biology, and medicine 2015; 11(5).

[62] Tautzenberger A, Kovtun A, Ignatius A. Nanoparticles and their potential for application in bone. In International journal of nanomedicine 2012; 7.

[63] Barry M, Pearce H, Cross L, Tatullo M, Gaharwar AK. Advances in Nanotechnology for the Treatment of Osteoporosis. In current osteoporosis reports 2016; 14(3).